Slow Warming of the Northern South China Sea during the Last Deglaciation

Tomoya Shintani[1], Masanobu Yamamoto[1, 2, *], and Min-Te Chen[3]

[1]Graduate School of Environmental Science, Hokkaido University, Sapporo, Japan
[2]Faculty of Environmental Earth Science, Hokkaido University, Sapporo, Japan
[3]Institute of Applied Geophysics, National Taiwan Ocean University, Keelung, Taiwan, ROC

ABSTRACT

We have generated a record of alkenone sea surface temperatures (SSTs) during the last 28000 years from Core MD97-2146 for the northern South China Sea (SCS). The SST record showed a typical pattern for change in the northern SCS SST. The SST during the LGM was ~25°C, this decreased to ~24°C to 17 ka, increased to ~25.5°C to 14.5 ka, decreased again to ~24.5°C to 11.8 ka, increased gradually to ~27°C to 6 ka, and then increased more gradually to reach ~27.5°C at present. The SST difference ($\Delta SST_{NSCS} = SST_{MD97-2146} - SST_{MD97-2141}$) between Cores MD97-2146 (the northern SCS; this study) and MD97-2141 (the Sulu Sea; Rosenthal et al. 2003) was used to characterize the SST changes in the northern SCS relative to changes in the adjacent WTP region. The ΔSST_{NSCS} decreased from 21 to 11.8 ka and increased after 11.8 ka, indicating slower warming of the northern SCS during the last deglaciation than that of the adjacent western tropical Pacific region. We infer that the slow warming of the northern SCS was principally a result of stronger winter monsoon during the last deglaciation and early Holocene. In addition, the cool water inflow through the Taiwan Strait after 13 ka and the warm water inflow through the Sunda Shelf after 11 ka could influence the SST in the northern SCS.

Key words: Alkenone, Sea surface temperature, South China Sea, MD97-2146, The last deglaciation, The last glacial maximum
Citation: Shintani, T., M. Yamamoto, and M. T. Chen, 2008: Slow warming of the northern South China Sea during the last deglaciation. Terr. Atmos. Ocean. Sci., 19, 341-346, doi: 10.3319/TAO.2008.19.4.341(IMAGES)

1. INTRODUCTION

The South China Sea (SCS) is a marginal sea of the North Pacific with seven connections to surrounding seas and oceans: the Taiwan Strait to the East China Sea (sill depth ~70 m), the Bashi Strait to the North Pacific (sill depth ~2500 m), the Mindoro and Balabac Straits to the Sulu Sea (sill depths ~450 and ~100 m, respectively), the Malacca Strait to the Indian Ocean (sill depth ~30 m), and the Gaspar and Karimata Straits (~40 - 50 m) to the Java Sea (Wyrtki 1961). Surface circulation in the SCS is driven by large-scale, seasonally-reversed monsoon winds (Wyrtki 1961). In the boreal summer, southwesterly winds drive an inflow of Indian Ocean water through the Sunda Shelf and a clockwise surface circulation in the SCS. In the boreal winter, north-easterly winds drive an inflow of North Pacific and East China Sea waters through the Bashi and Taiwan Straits, and

surface circulation in the SCS is counterclockwise.

Numerous paleoceanographic studies have been undertaken in the SCS. Wang and Wang (1990) and Wang et al. (1995) generated summer and winter sea-surface temperature (SST) records for the SCS based on foraminifer assemblages and demonstrated a larger seasonal SST difference and a larger latitudinal SST gradient during the last glacial maximum (LGM) than exist at present. Huang et al. (1997a, b) and Chen and Huang (1998) reported similar phenomena using foraminifer- and alkenone-based SST records for the northern SCS. Pelejero et al. (1999a) reported a larger latitudinal SST gradient during the LGM than that expressed at present, based on alkenone temperature records. Chen et al. (2003) applied a revised transfer function method (Mix et al. 1999) to winter and summer SST estimates and found a constant seasonal SST difference across glacial and interglacial cycles in the eastern SCS. Recently, Oppo and Sun (2005) and Zhao et al. (2006) reported millennium-scale

* Corresponding author
  E-mail: myama@ees.hokudai.ac.jp

temperature records from the northern and southern SCS, respectively, for the time since the penultimate glacial interval. The glacial and interglacial changes of SST in the SCS have been attributed either to the inflow of cool water from the North Pacific (e.g., Wang and Wang 1990; Wang et al. 1995) or to changes in winter monsoon intensity (e.g., Huang et al. 1997a, b).

This study presents a record of alkenone SSTs for the last 28000 years from Core MD97-2146 from the northern SCS offshore from China. The objective of this work is to understand changes in cooling caused by winter monsoon winds by comparing the reconstructed SCS SSTs with that of the Sulu Sea.

2. MATERIALS AND METHODS

During the IMAGES 1997 *Marion Dufresne* cruise, a giant piston core (MD97-2146; 38.69 m long) was collected from a water depth of 1720 m on the northern slope of the SCS at 20°07'N, 117°23'E (Fig. 1). The sediment retrieved consisted of dark gray nannofossil and foraminifer oozes with some radiolarians and diatoms (Chen et al. 1998).

An age model in calendar years was created from the AMS ^{14}C ages of 7 samples of the planktonic foraminiferan *Globigerinoides sacculifer* (Lin et al. 2006) and six samples of mixed planktonic foraminifera *Globigerinoides ruber* and *G. sacculifer*. The calendar age was converted using the CALIB5.0 program and marine04.14C dataset (Reimer et al. 2004) with a 400-year global reservoir correction (Table 1; Fig. 2). Lin et al. (2006) created an age model using a combination of ^{14}C ages and stratigraphic correlation with

nearby core 17940 (Wang et al. 1999). The present work does not use any stratigraphic correlation, however, because the assumption that temperatures in core 17940 changed synchronously with the Greenland temperature (Wang et al. 1999) is not necessarily valid.

A total of 74 samples were collected from levels up to a depth of 19 m (0 - 28 ka) in the core, every 20 cm on average (equivalent to approximately 300-year intervals). Alkenones were analyzed following the method of Yamamoto et al.
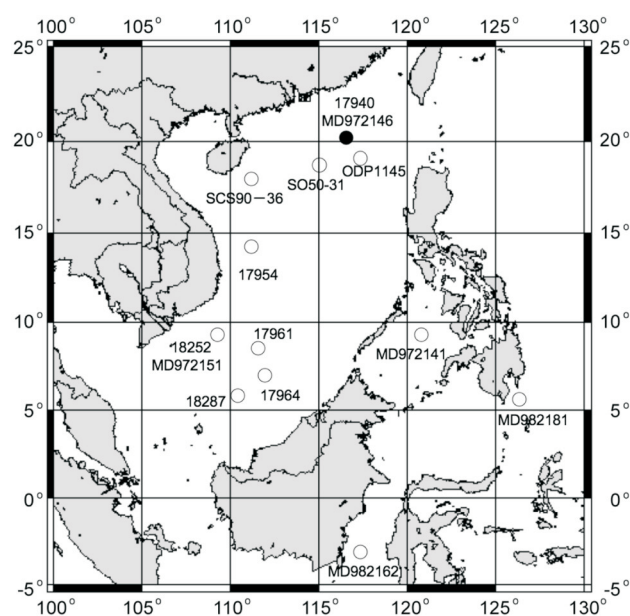

Fig. 1. Map showing the locations of Core MD97-2146 and other cores discussed in this paper.

Table 1. Age-depth model of core MD97-2146.

Depth (cm)	Method	Conventinal age (kyr BP)	Calendar age (kyr BP)	Reference
228.5	Mixed *G. ruber* and *G. sacculifer*	2.410 ± 0.035	2.04	This study
296.5	Mixed *G. ruber* and *G. sacculifer*	2.855 ± 0.035	2.64	This study
427.5	Mixed *G. ruber* and *G. sacculifer*	3.860 ± 0.040	3.82	This study
467.5	*G. sacculifer*	4.370 ± 0.080	4.52	Lin et al. (2006)
559.5	Mixed *G. ruber* and *G. sacculifer*	5.105 ± 0.170	5.46	This study
719.5	*G. sacculifer*	6.660 ± 0.060	7.20	Lin et al. (2006)
819.5	Mixed *G. ruber* and *G. sacculifer*	7.825 ± 0.050	8.30	This study
895.5	Mixed *G. ruber* and *G. sacculifer*	8.205 ± 0.050	8.70	This study
1051.5	*G. sacculifer*	10.090 ± 0.040	11.13	Lin et al. (2006)
1119.5	*G. sacculifer*	11.210 ± 0.040	12.83	Lin et al. (2006)
1365.5	*G. sacculifer*	14.460 ± 0.045	16.76	Lin et al. (2006)
1683.5	*G. sacculifer*	23.490 ± 0.080	27.17	Lin et al. (2006)
1911.5	*G. sacculifer*	24.440 ± 0.150	28.26	Lin et al. (2006)

Fig. 2. Age-depth model of Core MD97-2146.

Fig. 3. Alkenone temperature records from Core MD97-2146 for the last 30 kyr.

(2000) with an analytical accuracy of 0.24°C. Temperature was calculated following the methods of Prahl et al. (1988) and Pelejero and Grimalt (1997).

3. RESULTS AND DISCUSSION

3.1 Alkenone Temperatures from MD97-2146

Temperature records were calculated for core MD97-2146 using the equations of Prahl et al. (1988) with $U^{K'}_{37}$ and Pelejero and Grimalt (1997) with U^{K}_{37} (Fig. 3). The former temperatures were consistently ~0.7°C lower than the latter. Because the equation of Pelejero and Grimalt (1997) is more specific to SST estimation in the SCS, the temperatures obtained by using the Pelejero and Grimalt (1997) equation are used throughout the remainder of this paper.

The alkenone temperature during the LGM was ~25°C, this decreased to ~24°C at 17 ka, increased again to ~25.5°C to 14.5 ka, decreased to ~24.5°C to 11.5 ka, increased gradually to ~27°C to 6 ka, and then increased more gradually to reach ~27.5°C at present (Fig. 3). This variation was similar to that recorded in nearby core 17940 (Pelejero et al. 1999a). The core-top temperature was 26.8°C. This temperature agrees with the mean annual sea-surface temperature at this site (26.6°C; NOAA 1998).

3.2 Regional Patterns of SST Change in the South China Sea and the Adjacent Western Tropical Pacific Region

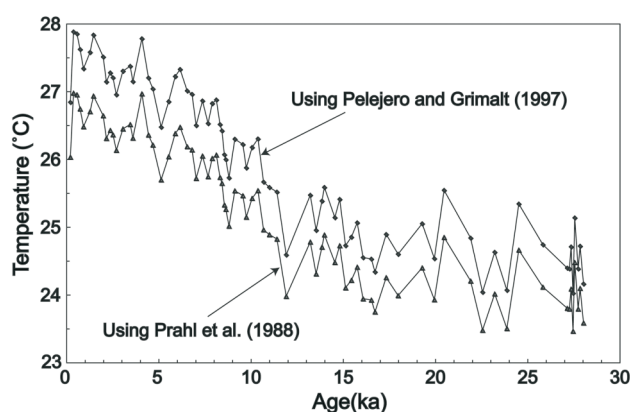The similar pattern of SST change in Core MD97-2146 was observed in the records of alkenone temperature and foraminifer-derived IKM and MAT winter temperatures at Cores SO50-31KL (Huang et al. 1997a) and SCS90-36 (Huang et al. 1997b; Fig. 4). ODP Site 1145 is located ~100 km south of Site MD97-2146, but the foraminiferal Mg/Ca-derived temperatures at ODP Site 1145 showed a pattern similar to those from the southern SCS, rather than those of other northern SCS cores (Oppo and Sun 2005).

Alkenone temperature records from the southern SCS exhibited a "Greenland-type" SST change in cores 17954 and 17946 (Pelejero et al. 1999a) and cores 18252-3 and 18287-3 (Kienast et al. 2001). SST varied between ~25°C and ~26°C from 21 to 15 ka, increased abruptly by ~1°C at ~15 ka, decreased by ~0.5°C to ~11.5 ka, increased gradually by 1 - 2°C to 5 ka, and then was nearly constant at ~28°C for the last 5 kyr (Fig. 4).

An "Antarctic type" SST change was reported from an alkenone temperature record from core 17954 off Vietnam in the western SCS (Pelejero et al. 1999a; Fig. 4). This type of SST change is also typical of the foraminiferal Mg/Ca-derived temperature records from the adjacent western tropical Pacific (WTP) region, such as core MD97-2146 in the Sulu Sea (Rosenthal et al. 2003), core MD98-02181 off Mindanao Island (Stott et al. 2002), and core MD98-2162 in the Makassar Strait (Visser et al. 2003). In this region, SST increased gradually by ~2.5°C from 20 to 11 ka, and then remained roughly constant or decreased slightly in the Holocene.

The temperature difference between the LGM and the present was ~3.5 - 4°C in the northern SCS and ~2.5°C in the southern SCS and the adjacent WTP region (Fig. 4). The northern SCS showed a greater temperature difference than did the other regions.

We used SST difference ($\Delta SST_{NSCS} = SST_{MD97-2146} - SST_{MD97-2141}$) between Cores MD972146 (the northern SCS; this study) and MD97-2141 (the Sulu Sea; Rosenthal et al. 2003) and the SST difference ($\Delta SST_{SSCS} = SST_{17961} - SST_{MD97-2141}$) between Cores 17961 (the southern SCS; Pelejero et al. 1999a) and MD97-2141 (the Sulu Sea), in order to characterize the regional differences of SST

Fig. 5. Changes in the SST difference (ΔSST_{NSCS}) between Cores MD972146 (the northern SCS; this study) and MD97-2141 (the Sulu Sea; Rosenthal et al. 2003) and ΔSST_{SSCS} between Cores 17961 (the southern SCS; Pelejero et al. 1999) and MD97-2141.
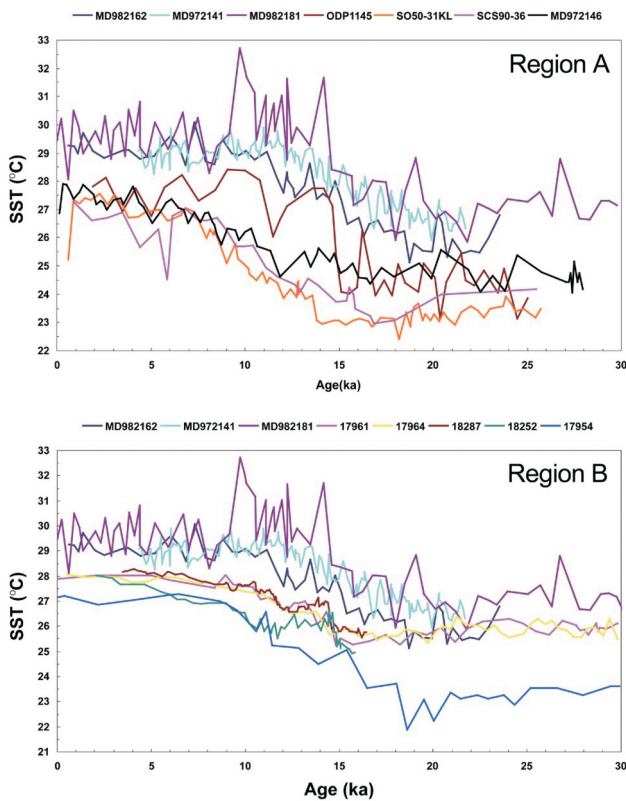
Fig. 4. Comparison of alkenone- and foraminiferal Mg/Ca-derived SST records from the South China Sea and the adjacent western tropical Pacific region. Region A: SSTs from the northern SCS and the adjacent western tropical Pacific region. Region B: SSTs from the southern and western SCS and the adjacent western tropical Pacific region. Data from Huang et al. (1997a) for Core SO50-31KL, Huang et al. (1997b) for Core SCS90-36, Pelejero et al. (1999a) for Cores 17954, 17961, and 17964, Kienast et al. (2001) for Cores 18252 and 18287, Stott et al. (2002) for Core MD98-2181, Rosenthal et al. (2003) for Core MD97-2141, Visser et al. (2003) for Core MD98-2162, and Oppo and Sun (2005) for ODP Site 1145.

changes in the SCS relative to changes in the adjacent WTP region.

The ΔSST_{NSCS} decreased gradually from ~21 ka, reached a minimum at ~11.8 ka, and then gradually increased (Fig. 5). The ΔSST_{SSCS} decreased gradually from ~19 ka and reached a minimum at ~15 ka. It abruptly increased after ~15 ka, was nearly constant from ~14.5 to ~11 ka, and increased gradually after ~11 ka (Fig. 5). Changes in these two temperature-difference parameters indicate that warming of the SCS lagged behind that of the adjacent WTP region during early deglaciation. At ~15 ka, the southern SCS abruptly warmed and started to follow the warming trend of the adjacent WTP region. In contrast, the warming of the northern SCS was less pronounced at ~15 ka, and the ΔSST_{NSCS} decreased after ~15 ka. The northern SCS is characterized by slower warming during the last deglaciation than the southern SCS and the adjacent WTP region.
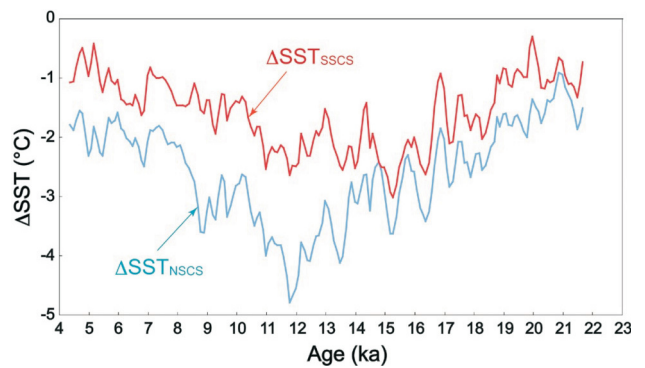
3.3 Hydrographic Changes in the South China Sea Since the Last Glacial Maximum

Three distinct domains of changing SSTs have been identified. The SST of the WTP region increased first, during early deglaciation. The early deglacial warming in the WTP was most likely a hemispheric climatic response to orbital forcing (Rosenthal et al. 2003; Visser et al. 2003). The near absence of this response in the SCS is attributed to its specific hydrographic conditions. During the LGM, the SCS was a semi-isolated sea connected to the North Pacific through the Bashi Strait, and to the Sulu Sea through the narrow Mindoro Strait. The SCS was linked to the East China Sea through the Taiwan Strait (sill depth ~70 m) only after ~13 ka, and to the Java Sea through the Gaspar and Karimata Straits (~40 - 50 m) after ~11 ka. Wang and Wang (1990) suggested that temperate waters intruded into the SCS through the Bashi Strait from the North Pacific during the LGM, and circulated counterclockwise within the SCS under the influence of winter monsoon winds. This hypothesis was proposed to explain why a larger latitudinal temperature gradient existed in the SCS during the LGM than at present (e.g., Wang and Wang 1990; Wang et al. 1995; Pelejero et al. 1999a). In contrast, Huang et al. (1997a, b) proposed that an intensified winter monsoon during the LGM cooled the SSTs and enhanced marine productivity in the SCS by mixing surface water. The SST of the Kuroshio Current was estimated to be ~25 - 26°C offshore of Taiwan during the LGM (Chen et al. 1992). This SST was as high as those of the northern SCS (~25°C) and the southern SCS (~25 - 26°C). Huang et al. (1997a, b) pointed out that the inflow of North Pacific water must not be effective in cooling the SST of the SCS. The stronger winter monsoon during the LGM most likely resulted in cooler SSTs and a large latitudinal SST gradient in the SCS. The same hydrographic and atmospheric conditions would maintain cooler condi-

tions in the SCS during the early deglaciation, even as the adjacent western Pacific region started warming. The contrast of SST trends between the SCS and the Sulu Sea suggests that only a restricted exchange of water was possible between the seas through the Mindoro Strait.

At ~15 ka, the southern SCS abruptly warmed and began to follow the warming trend of the adjacent WTP region, but warming of the northern SCS was less pronounced. After ~15 ka, the latitudinal temperature gradient in the SCS increased, reaching a maximum at ~12 ka, and then decreased to the present level by ~6 ka (Fig. 4). The abrupt warming of the southern SCS was not the result of a weakened winter monsoon. The weakening of the winter monsoon likely caused warming of both the southern and northern SCS, but warming of the northern SCS was not as significant. Pelejero et al. (1999b) suggested that this might have been because sea-level rise caused the development of a vast, shallow warm-water pool over the Sunda Shelf during this interval and enhanced the SSTs in the SCS. In contrast, the northern SCS remained cool under the influence of intensified winter monsoons.

After 13 ka, the Taiwan Strait was open. China Coastal Water (CCW) could flow into the SCS through the Taiwan Strait, as is common in winter at present. The large latitudinal SST gradient in the SCS after ~13 ka is attributed partly to the increased inflow of cool CCW. The gradual decrease of the latitudinal SST gradient in the SCS from ~12 to ~6 ka can be attributed to the gradual weakening of the winter monsoon associated with the decrease of the cool CCW inflow or the increased inflow of the tropical Indian Ocean water into the SCS through the Sunda Shelf.

The decreasing trend of ΔSST_{NSCS} from 21 to 11.8 ka suggests the gradual intensification of the winter monsoon. In the same sense, the decreasing trend of ΔSST_{NSCS} after 11.8 ka is attributed to the gradual weakening of the winter monsoon or the increased flow of tropical Indian Ocean water into the SCS through the Sunda Shelf. Although there is little evidence of winter monsoon changes during the last deglaciation, An (2000) argued that the higher dust deposition rates in the central Loess Plateau of China during the early Holocene (~5 - 10 ka) reflect a stronger winter monsoon. Ueshima et al. (2006) also suggested that the intensity of the Aleutian Low varied in response to the Earth's obliquity (~41-kyr cycle) and was maximized at ~10 ka, based on 145-kyr organic carbon records from the Kuroshio-Oyashio transition zone off central Japan. The minimum winter insolation at northern high latitudes at ~10 ka may have enhanced the Siberian High. The temperature contrast between Siberia and the warming tropical Pacific created favorable conditions for a stronger winter monsoon. We infer that the intensity of the East Asian winter monsoon was linked to high-latitude atmospheric circulation, and the intensified winter monsoon caused the slow deglacial warming of the northern SCS.

4. CONCLUSIONS

The 28-kyr SST records from Core MD97-2146 showed a typical northern SCS SST changing pattern. The SST difference ($\Delta SST_{NSCS} = SST_{MD97-2146} - SST_{MD97-2141}$) between the northern SCS and the Sulu Sea was used to characterize the SST changes in the northern SCS relative to changes in the adjacent WTP region. The ΔSST_{NSCS} decreased from 21 to 11.8 ka and increased after 11.8 ka, indicating a slow warming of the northern SCS during the last deglaciation. We infer that the slow warming was principally a result of stronger winter monsoon during the last deglaciation and the early Holocene. In addition, the cool water inflow through the Taiwan Strait after 13 ka and the warm water inflow through the Sunda Shelf after 11 ka could influence the SST in the northern SCS.

REFERENCES

An, Z. S., 2000: The history and variability of the East Asian paleomonsoon climate. *Quat. Sci. Rev.*, **19**, 171-187.

Chen, M. P., C. K. Huang, L. Lo, and C. H. Wang, 1992: Late Pleistocene paleoceanography of the Kuroshio Current in the area offshore Southeast Taiwan. *Terr. Atmos. Ocean. Sci.*, **3**, 81-110.

Chen, M. T. and C. Y. Huang, 1998: Ice-volume forcing of winter monsoon climate in the South China Sea. *Paleoceanography*, **13**, 622-633.

Chen, M. T., L. Beaufort, and the Shipboard Scientific Party of the IMAGES III/MD106-IPHIS Cruise (Leg II), 1998: Exploring Quaternary variability of the East Asian monsoon, Kuroshio Current, and the Western Pacific warm pool systems: High-resolution investigations of paleoceanography from the IMAGES III/MD106-IPHIS cruise. *Terr. Atmos. Ocean. Sci.*, **9**, 129-142.

Chen, M. T., L. J. Shiau, P. S. Yu, T. C. Chiu, Y. G. Chen, and K. Y. Wei, 2003: 500000-Year records of carbonate, organic carbon, and foraminiferal sea surface temperature from the southeastern South China Sea (near Palawan Island). *Palaeogeogr. Palaeoclimatol. Palaeoecol.*, **197**, 113-131.

Huang, C. Y., P. M. Liew, M. Zhao, T. C. Chang, C. M. Kuo, M. T. Chen, C. H. Wang, and L. Zheng, 1997a: Deep sea and lake records of the Southeast Asian paleomonsoons for the last 25 kyrs. *Earth Planet. Sci. Lett.*, **146**, 59-72.

Huang, C. Y., S. F. Wu, M. Zhao, M. T. Chen, C. H. Wang, X. Tu, and P. B. Yuan, 1997b: Surface ocean and monsoon climate variability in the South China Sea since last

glaciation. *Mar. Micropaleontol.*, **32**, 71-94.

Kienast, M., S. Steinke, K. Stattegger, and S. E. Calvert, 2001: Synchronous tropical South China Sea SST changes and Greenland warming during deglaciation. *Science*, **291**, 2132-2134.

Lin, D. C., C. H. Liu, T. H. Fang, C. H. Tsai, M. Murayama, and M. T. Chen, 2006: Millennial-scale changes in terrestrial sediment input and Holocene surface hydrography in the northern South China Sea. *Palaeogeogr. Palaeoclimatol. Palaeoecol.*, **236**, 56-73.

Mix, A. C., A. E. Morey, and N. G. Pisias, 1999: Foraminiferal fauna estimates of paleotemperature: Circumventing the no-analog problem yields cool ice age tropics. *Paleoceanography*, **14**, 350-359.

NOAA, 1998: http://iridl.ldeo.columbia.edu/SOURCES/.NOAA /.NODC/.WOA98/.

Oppo, D. W. and Y. Sun, 2005: Amplitude and timing of sea-surface temperature changes in the northern South China Sea: Dynamic link to the East Asian monsoon. *Geology*, **33**, 785-788.

Pelejero, C. and J. O. Grimalt, 1997: The correlation between the $U^{K'}_{37}$ index and sea surface temperatures in the warm boundary: The South China Sea. *Geochim. Cosmochim. Acta*, **61**, 4789-4797.

Pelejero, C., J. O. Grimalt, S. Heilig, M. Kienast, and L. Wang, 1999a: High-resolution $U^{K'}_{37}$ temperature reconstructions in the South China Sea over the past 220 kyr. *Paleoceanography*, **14**, 224-231.

Pelejero, C., M. Kienast, L. Wang, and J. O. Grimalt, 1999b: The flooding of Sundaland during the last deglaciation: Imprints in hemipelagic sediments from the southern South China Sea. *Earth Planet. Sci. Lett.*, **171**, 661-671.

Prahl, F. G., L. A. Muehlhausen, and D. L. Zahnle, 1988: Further evaluation of long-chain alkenones as indicators of paleoceanographic conditions. *Geochim. Cosmochim. Acta*, **52**, 2303-2310.

Reimer, P. J., M. G. L. Baillie, E. Bard, A. Bayliss, J. W. Beck, C. J. H. Bertrand, P. G. Blackwell, C. E. Buck, G. S. Burr, K. B. Cutler, P. E. Damon, R. L. Edwards, R. G. Fairbanks, M. Friedrich, T. P. Guilderson, A. G. Hogg, K. A. Hughen, B. Kromer, F. G. McCormac, S. W. Manning, C. B. Ramsey, R. W. Reimer, S. Remmele, J. R. Southon, M. Stuiver, S. Talamo, F. W. Taylor, J. van der Plicht, and C. E. Weyhenmeyer, 2004: IntCal04 terrestrial radiocarbon age calibration, 0 - 26 Cal Kyr BP. *Radiocarbon*, **46**, 1029-1058.

Rosenthal, Y., D. W. Oppo, and B. K. Linsley, 2003: The amplitude and phasing of climate change during the last deglaciation in the Sulu Sea, western equatorial Pacific. *Geophys. Res. Lett.*, **30**, 1428.

Stott, L., C. Poulsen, S. Lund, and R. Thunell, 2002: Super ENSO and global climate oscillations at millennial time scales. *Science*, **297**, 222-226.

Ueshima, T., M. Yamamoto, T. Irino, T. Oba, M. Minagawa, H. Narita, and M. Murayama, 2006: Long term Aleutian Low dynamics and obliquity-controlled oceanic primary production in the mid-latitude western North Pacific (Core MD01-2421) during the last 145000 years. *Global Planet. Change*, **53**, 21-28.

Visser, K., R. Thunell, and L. Stott, 2003: Magnitude and timing of temperature change in the Indo-Pacific warm pool during deglaciation. *Nature*, **421**, 152-155.

Wang, L. and P. Wang, 1990: Late Quaternary paleoceanography of the South China Sea: Glacial-interglacial contrasts in an enclosed basin. *Paleoceanography*, **5**, 77-90.

Wang, L., M. Sarnthein, H. Erlenkeuser, J. O. Grimalt, P. M. Grootes, S. Heilig, E. Ivanova, M. Kienast, C. Pelejero, and U. Pflaumann, 1999: East Asia monsoon climate during the late Pleistocene: high-resolution sediment records from the South China Sea. *Mar. Geol.*, **156**, 245-284.

Wang, P., L. Wang, Y. Bian, and Z. Jian, 1995: Late Quaternary paleoceanography of the South China Sea: surface circulation and carbonate cycles. *Mar. Geol.*, **127**, 145-165.

Wyrtki, K., 1961: Physical oceanography of the southeast Asia waters. In: Scientific Results of Maritime Investigations of the South China Sea and the Gulf of Thailand 1959-1961, Naga Rep. 2, Scripps Inst. Oceanogr., La Jolla, Calif. USA.

Yamamoto, M., M. Yamamuro, and R. Tada, 2000: Late Quaternary records of organic carbon, calcium carbonate and biomarkers from Site 1016 off Point Conception, California margin. *ODP Scientific Results*, **167**, 183-194.

Zhao, M., C. Y. Huang, C. C. Wang, and G. Wei, 2006: A millennial-scale $U^{K'}_{37}$ sea surface temperature record from the South China Sea (8°N) over the last 150 kyr: Monsoon and sea-level influence. *Palaeogeogr. Palaeoclimatol. Palaeoecol.*, **236**, 39-55.